

Surface modification of TiO₂ nanoparticles with AHAPS aminosilane: distinction between physisorption and chemisorption

Mounir Kassir · Thibault Roques-Carmes ·
Tayssir Hamieh · Angelina Razafitianamaharavo ·
Odile Barres · Joumana Toufaily · Frédéric Villiéras

Received: 26 March 2013 / Accepted: 12 June 2013 / Published online: 25 June 2013
© Springer Science+Business Media New York 2013

Abstract This paper addresses the surface modification of TiO₂ nanoparticles with *n*-(6-aminohexyl) aminopropyltrimethoxysilane (AHAPS) using various initial aminosilane concentrations. The main objective of this article is to show experimentally the importance of the physisorption during the grafting process. The distinction between chemisorbed and physisorbed aminosilane molecules on TiO₂ is thoroughly analyzed. The surface of bare and modified TiO₂ particles has been characterized by Fourier transform infrared spectroscopy (FTIR) and X-ray photoelectron spectroscopy (XPS) to gain a better understanding of the adsorption mechanism of AHAPS on TiO₂. Quantitative information on surface energy of TiO₂, in terms of adsorption energy sites and heterogeneity, has

been investigated by quasi-equilibrium low-pressure adsorption technique using nitrogen and argon as probe molecules. The FTIR and XPS data are combined to estimate and discuss the chemisorbed and physisorbed contribution. The results demonstrate that both physisorption and chemisorption occurs but they display a different behavior. The physisorbed amounts are much higher than the chemisorbed amounts. This shows that the main part of the adsorbed layer is composed of physisorbed molecules. The physisorbed uptake depends highly on the AHAPS concentration while the chemisorbed amount remains constant. Quasi-equilibrium Ar derivative adsorption isotherms reveal that the AHAPS molecules are mostly located on the {101} and {001} faces of titania and that the two faces display the same reactivity toward AHAPS sorption. Nitrogen adsorption experiments show that the sorption takes place on the three polar surface sites of high energy. The molecules are chemisorbed onto the site displaying the highest energy while they are physisorbed on the two lower energy sites.

Electronic supplementary material The online version of this article (doi:10.1007/s10450-013-9555-y) contains supplementary material, which is available to authorized users.

M. Kassir · A. Razafitianamaharavo · F. Villiéras
Laboratoire Interdisciplinaire des Environnements Continentaux,
Université de Lorraine, UMR 7360, CNRS, 15 Avenue du
Charmois, 54500 Vandœuvre-lès-Nancy, France

M. Kassir · T. Hamieh · J. Toufaily
Laboratory of Materials, Catalysis, Environment and Analytical
Methods, Faculty of Sciences I, Lebanese University,
Campus Rafic Hariri, Beyrouth, Lebanon

T. Roques-Carmes (✉)
Laboratoire Réactions et Génie des Procédés, Université de
Lorraine, UPR 3349, CNRS, 1 rue Grandville, 54001 Nancy
Cedex, France
e-mail: thibault.roques-carmes@univ-lorraine.fr

O. Barres
GeoRessources, Université de Lorraine, UMR 7359, CNRS,
CREGU, Faculté des Sciences et Techniques, Rue Jacques
Callot, 54506 Vandœuvre-lès-Nancy, France

Keywords Aminosilane coupling agent · Surface modification · TiO₂ nanoparticles · Low-pressure argon and nitrogen adsorption · Physisorption · Chemisorption

1 Introduction

Titanium dioxide is a very important semiconductor with a high potential for applications in solar cells (Grätzel 2001), photocatalysis (Herrmann 2010; Blin et al. 2012), biomedical devices (Brunette et al. 2001), sensing, and various other areas of nanotechnology. Over the last decades, increasing attention has been focused on the modification of the TiO₂ surface with organosilane molecules.

Grafting active functional groups onto particle surface can increase the possibility of chemical bonds formation between modified particles and fabrics in order to assemble various molecules and materials thereby improving their adhesion strength. Amino-terminated organosilane molecules are of particular interest due to their chemical reactivities. They have been applied to anchor metal catalysts (Brandow et al. 1999), polymers (Petri et al. 1999), biomolecules such as enzymes (Harnett et al. 2001; Oh et al. 2002), proteins (Lee et al. 2009; Aldeek et al. 2011) and DNA (Kneuer et al. 2000; Wu et al. 2011) onto TiO₂. The chemical selectivity of an amino-terminated grafted monolayer is based on the formation of specific chemical bonds or electrostatic attractive forces between the terminal amino groups of the grafted layer and the functional groups of the adsorbate (biomolecules, DNA). For instance, carboxyl, aldehyde and sulfonic acid groups interact strongly with amino groups.

A particular problem related to aminosilane attachment on TiO₂ is the tendency to form multilayers instead of the desired monolayer (Zheng et al. 2000). The first layer is generally composed of chemisorbed silane adsorbed on the surface via covalent bond (chemisorption). The second layer appears as a physisorbed layer which is a loosely bound layer over the chemisorbed layer. Another specific issue which needs to be addressed is the coadsorption of physisorbed aminosilane molecules with the grafted (chemisorbed) molecules in the first layer (Vandenberg et al. 1991). The aminosilane attachment and orientation respond to different reaction conditions and methods. The aminosilane could link to the oxide surface not only by a covalent bond (chemisorption) with free amine groups away from the surface, but also by hydrogen-bond between the amine and the surface, or by electrostatic attachment between the protonated amine and the negatively charged titania surface (Ukaji et al. 2007; Zhao et al. 2011).

However, for using amino-terminated molecules in the above applications (sensor for DNA detection, adhesion of protein...), a controlled chemisorption and absence of physisorbed molecules are required. The physisorbed molecules can be removed by contact with solvent for several hours at room temperature (Hoogeveen et al. 1996; Roques-Carnes et al. 2006; Jansson et al. 2010). For instance, Zhao et al. used the following washing procedure to eliminate the excess of physisorbed aminosilane molecules from TiO₂ nanoparticles: washing with ethanol and water alternatively for at least two cycles (Zhao et al. 2011). Some previous measurements indicate that aminosilane physisorption on oxides is only partially reversible (Weigel and Kellner 1989) since 3–10 % of the total physisorbed amount can remain on the surface after the rinsing process.

Very few studies have directly addressed the contribution of physisorbed aminosilane molecules during the

organosilane grafting process on titania. Experimentally, this competition between the chemisorption and physisorption is expected to produce a decrease in the chemisorbed amount at a certain critical coverage value. An example of this will be given in the following study. The main objective of this paper is to show experimentally the importance of the physisorption during the aminosilane grafting process on titania by measuring its contribution in the adsorption layer. For this reason, the distinction between chemisorbed and physisorbed aminosilane molecules on TiO₂ is thoroughly examined. Aminopropyltriethoxysilane (APTES) and *n*-(6-aminoethyl)aminopropyltrimethoxysilane (AHAPS) are among the aminosilanes currently most commonly used as coupling agents to functionalize the surface of titania. The presence of the amine group in the chain of APTES and AHAPS plays a key role in the adsorption reaction. Overall, while some very useful aspects of APTES grafting on TiO₂ have been studied (Ukaji et al. 2007; Zhao et al. 2011) and reaction details have been further elucidated on SiO₂ surface (Lazghab et al. 2010; Yang et al. 2012), a systematic study of AHAPS grafting on TiO₂ have not been reported. Therefore, the present work explores the surface modification of TiO₂ nanoparticles with AHAPS using various initial aminosilane concentrations to obtain different surface coverage. The surface of pure anatase TiO₂ nanoparticles is chemically modified using AHAPS according to the classical procedure reported in the literature (Ukaji et al. 2007; Zhao et al. 2011). However, no washing procedure is performed in order to maintain the physisorbed molecules onto the surface. It becomes then possible to monitor, *in situ*, the amount of molecules physisorbed during the grafting. The surface of the modified TiO₂ particles has been characterized by Fourier transform infrared spectroscopy (FTIR) and X-ray photoelectron spectroscopy (XPS) to gain a better understanding of the adsorption mechanism of AHAPS on TiO₂. Quantitative information on surface energy of TiO₂, in terms of adsorption energy sites and heterogeneity, has been investigated by quasi-equilibrium low-pressure adsorption technique using nitrogen and argon as probe molecules.

2 Materials and methods

2.1 Titania nanoparticles

Titanium dioxide (99 % purity) of BET (N₂) specific surface area (S) equals to 157 ± 3.7 m²/g was purchased from Iolitec. This titania was used without additional purification. As powder solid, this titania was chosen due to its low porosity and small particle size. The particle size of the nanoparticles had been determined by transmission electron microscopy (TEM), surface area analysis (BET) and X-ray diffraction peak broadening analysis (XRD).

For spherical particles with a narrow size distribution, the specific surface area provides an average particle diameter d according to (Bowen 2002):

$$d = \frac{6}{\rho \times S} \quad (1)$$

where S is the specific surface area and ρ the theoretical density. Calculation using Eq. (1) leads to a mean particle size of 11 nm.

Powder X-ray diffraction (XRD) analyses were obtained using Panalytical X'Pert Pro MPD diffractometer using Cu $K\alpha$ radiation. Figure 1 displays the XRD pattern of the TiO_2 particles. The curve shows typical pattern of the anatase powder of good quality (good crystallinity). The peaks corresponding to the anatase structure can be seen at 29.5° (101), 44.3° (004) and 56.1° (211) in 2θ . All peaks are in good agreement with the standard spectrum (JCPDS no.: 84-1286). This emphasizes that anatase is the only formed phase. Note that the reflection of the {001} face cannot be directly detected but is confirmed by the occurrence of the (004) peak. The broadening of the anatase diffraction peaks is attributed to the nanometer size of the particles and can be used to determine the mean particle size. From the well-known Scherrer formula the average crystallite size, L , is:

$$L = \frac{K\lambda}{\beta \cos\theta} \quad (2)$$

where λ is the X-ray wavelength, β is the peak width of the diffraction peak profile at half maximum height resulting from small crystallite size and K is a constant related to crystallite shape, normally taken as 0.9. Under our condition, L represents the length of the coherent scattering domain according to the angle θ where it corresponds to the size of particles. Calculation using Scherrer formula (Eq. 2) gives a particle size of 12 nm.

The average particle diameter was also estimated to be 5–20 nm by TEM. This size value correlated well with the results obtained from XRD analysis (12 nm) and BET analysis (11 nm). The nanoparticles were not spherical but displayed a bipyramidal shape (TEM). More precisely, more or less elongated bipyramids were observed. In addition the high resolution micrograph indicated that the particles were elongated in the [001] direction and exposed the (101) surfaces as proposed by Durupthy et al. (2007).

2.2 Surface modification of TiO_2 nanoparticles

The surface of TiO_2 was chemically modified using the aminosilane AHAPS. The chemicals used for the surface modification included *n*-(6-aminohexyl) aminopropyltrimethoxysilane ($H_2N(CH_2)_6NH(CH_2)_3Si(OCH_3)_3$, AHAPS), supplied by Gelest Inc. (purity 95 %),

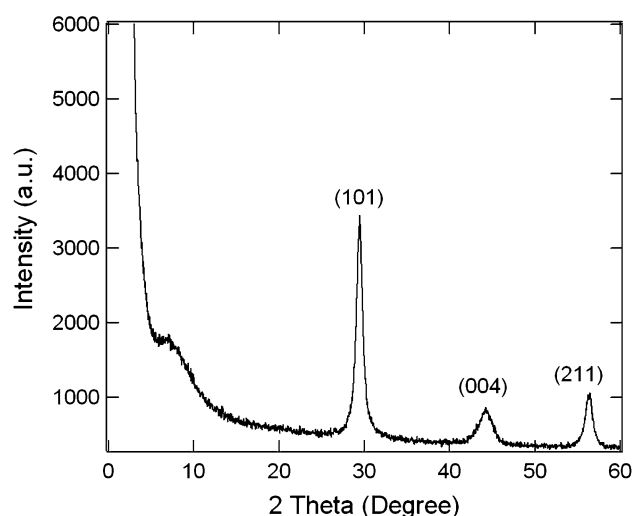


Fig. 1 X-ray diffraction pattern of TiO_2 Iolitec

and ethanol (Sigma-Aldrich, 99.9 %). The dry powder was placed in a drying oven at $210^\circ C$ during 4 h. Afterward, 1 g of powder was dispersed into 20 mL of ethanol solution containing AHAPS at different initial concentrations ranging from 0.05 to 9 mM. After 10 h of stirring at room temperature, the reaction was stopped. Then, the particles were separated from the solvent by decantation. The titania precipitates were washed once with ethanol. Note that no washing procedure was performed in order to reduce as much as possible the desorption of the physisorbed molecules from the surface. Finally, the particles were dried in a drying oven maintained at $130^\circ C$ for 10 h in order to remove ethanol.

The thermal analysis of the modified TiO_2 particles was carried out in order to demonstrate the thermal stability of the adsorbed AHAPS molecules in the temperature range from 20 to $300^\circ C$ (Rate thermal analysis coupled with mass spectrometry, not shown). The results showed that the AHAPS molecules on the surface were stable up to $300^\circ C$. This emphasizes that the solid–gas experiments (outgassing at $110^\circ C$) can be safely carried out without deterioration of the AHAPS molecules.

2.3 Surface characterization of modified TiO_2 nanoparticles

Several measurements were made on solid samples in order to characterize the modification of the titania surface: FTIR, XPS and low-pressure argon and nitrogen adsorption.

Diffuse reflectance spectra were recorded using a Fourier transform infrared spectrometer (BRUKER IFS 55) equipped with a large-band mercury cadmium telluride (MCT) detector cooled at 77 K and associated with a diffuse reflectance attachment (Harrick Corporation). The sample preparation involved the mixing of the solid sample

with KBr (potassium bromide). Each sample was scanned 200 times (around 2 min) and the influence of atmospheric water and carbon dioxide was subtracted.

XPS measurements were performed at a residual pressure of 10^{-9} mbar, using a KRATOS Axis Ultra electron energy analyzer operating with an Al K α monochromatic source (LCPME, Université de Lorraine, CNRS). A rotating anode served to generate an Al K α X-ray beam of 7.6 kW (photon energy of 1,486 eV). The X-ray beam was monochromated using seven bent quartz crystals and focused onto the sample resting on an automated goniometer. The detector system consisted of a 300 mm mean radius hemispherical energy analyzer and a multichannel plate detector and provided an overall energy resolution of 0.27 eV as determined at room temperature by the Fermi level edge of Ag.

Energetic heterogeneity of solid surfaces was examined using low-pressure quasi-equilibrium adsorption. Low pressure isotherms of argon and nitrogen at 77 K were recorded on a lab-built automatic quasi-equilibrium volumetric set-up (Villieras et al. 1992, 1997, 1998; Michot et al. 1990). High purity argon and nitrogen (>99.9995 %, Alphagaz) were used. The solid sample (around 700 mg) was outgassed under a residual pressure of 10^{-4} Pa overnight at 120 °C to remove physisorbed water molecules and other impurities. After outgassing, a slow, constant, and continuous flow of adsorbate was introduced into the adsorption cell through a micro-leak. The flow rate was constant, at least up to the BET domain, and can be adjusted by the pressure imposed before the leak. Since the introduction rate was low enough, the measured pressures were considered as quasi-equilibrium pressures (in the range of 10^{-3} – 3×10^4 Pa) (Michot et al. 1990; Villieras et al. 1998). Then, the adsorption isotherm was derived by recording the quasi-equilibrium pressure as a function of time. From the recording of quasi-equilibrium pressure as a function of time, high resolution adsorption isotherms were obtained with more than 2,000 data points for the filling of the first monolayer (relative pressure P/P_0 lower than 0.15). Due to the large number of experimental data points, the experimental derivative of the adsorbed quantity could be calculated as a function of the logarithm of the relative pressure ($\ln(P/P_0)$) which corresponds to the free energy adsorption expressed in kT units (Villieras et al. 1992, 1997, 1998; Stephanovic et al. 2010). The derivative of an adsorption isotherm was much more sensitive to surface heterogeneity since it featured slight variations and appearance of domains. Derivative isotherms can then be simulated using theoretical derivative adsorption isotherms by applying the so-called derivative isotherm summation (DIS) method. An excellent description and detailed discussion of the DIS method can be found in the literature (Villieras et al. 1997, 2002; Prelot et al. 2003; Stephanovic et al. 2010).

Each local isotherm was characterized by three parameters: the peak position ($\ln(P/P_0)$) related to the interaction between the surface and an adsorbed molecule, the lateral interactions (ω) between two neighboring adsorbed molecules, and the monolayer capacity (amount of gas adsorbed V_m) on a given domain. The ω parameter was also used as an adjustable parameter allowing the correct modeling of the derivative widths. It depended on both the physical lateral interactions between two neighboring adsorbed molecules and the distribution of normal interactions between the adsorbed molecule and the surface (reflecting the energy heterogeneity of the given domain). The specific area (S) of each domain was obtained from the amount of gas adsorbed V_m . Various adsorption sites can be evidenced depending on the nature of the adsorbed gas, such as argon or nitrogen. The first one revealed mostly structural sites, whereas the second one may probe for specific interactions with the surface sites due to its polarizability (i.e. the quadrupolar momentum).

3 Results and discussion

3.1 FTIR results and discussion

The Fig. 2 shows the FTIR spectra of bare and modified TiO₂ prepared at various initial AHAPS concentrations. After surface modification by aminosilane, the appearance of two absorption peaks between 3,000 and 2,750 cm⁻¹, assigned to the stretching of CH₃ and CH₂ groups, is evidenced. They indicate the presence of the carbon chains of the organosilane molecules. In addition, a small shoulder appears around 1,560 cm⁻¹, which corresponds to the N–H bending vibration of primary amines (NH₂) at the functional amino group. This demonstrates that amine functional groups of the organosilane exist on the particle surface. According to the FTIR analysis, it could be concluded that the aminosilane coupling agent is successfully adsorbed onto the surface of TiO₂ nanoparticles. For all the samples (bare and modified titania), the stretching vibration of adsorbed water is confirmed by the broad absorption band between 3,400 and 3,200 cm⁻¹. The band corresponding to the surface hydroxyl groups (–OH) on the TiO₂ surface is observed at 3,600–3,400 cm⁻¹, because of overlapping with the band related to physically adsorbed water on the TiO₂ surface. In the presence of AHAPS on the surface, a significant decrease of the band corresponding to the surface hydroxyl groups is reported indicating the interaction of these molecules with the surface hydroxyl groups. This confirms the chemical adsorption (chemisorption) of AHAPS molecules on the surface. It is then anticipated that the silanation reaction of AHAPS with surface hydroxyl groups takes place with a two-step

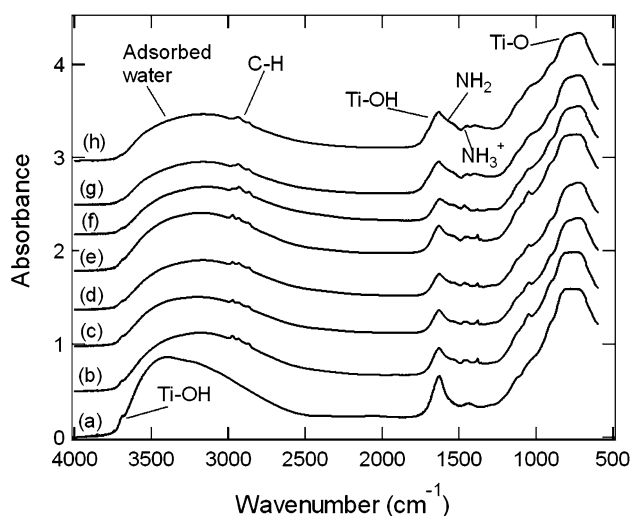
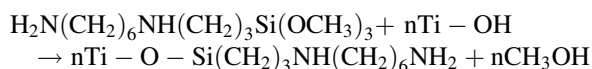


Fig. 2 Infrared spectra of bare and modified TiO₂ for initial AHAPS concentrations of: *a* 0 mM, *b* 0.05 mM, *c* 0.5 mM, *d* 1 mM, *e* 2 mM, *f* 3 mM, *g* 5 mM and *h* 9 mM

mechanism. Some of the AHAPS are hydrolysed first. This step leads to the release of methanol. Then, the hydrolyzed reagent comes into contact with hydroxyl groups of the solid surface and is grafted on it. The substitution reaction can be summarized as:



where *n* is the number of bonds between the AHAPS molecule and the surface hydroxyl groups.

The chemical modification is studied using the band corresponding to the surface hydroxyl group (3,600–3,400 cm⁻¹). We aim to estimate, semi-quantitatively, the amount of AHAPS chemisorbed at the surface of titania by integrating the area under the band. A baseline correction is necessary prior to the integration of the area under the band. The AHAPS grafting of TiO₂ reduces the concentration of surface hydroxyl groups and also the area under the band. Figure 3 depicts the area under the band (surface hydroxyl) as a function of the AHAPS initial concentration. Note that each value reported in the figure is an average of three measurements. Data are considered acceptable only if for three repetitions, the data for each point differ by less than 5 %. The area decreases with the AHAPS concentration up to a pseudo-plateau observed for a concentration close to 2 mM. More precisely, the adsorption trend divides in three principal parts. At low AHAPS concentration (up to a concentration of 0.05 mM) the area drops strongly (increase of chemisorption). At higher AHAPS concentrations, starting at 0.05 mM, the area decreases slightly up to a pseudo-plateau. At AHAPS concentrations larger than or equal to 2 mM, the area becomes roughly constant. The presence of the plateau

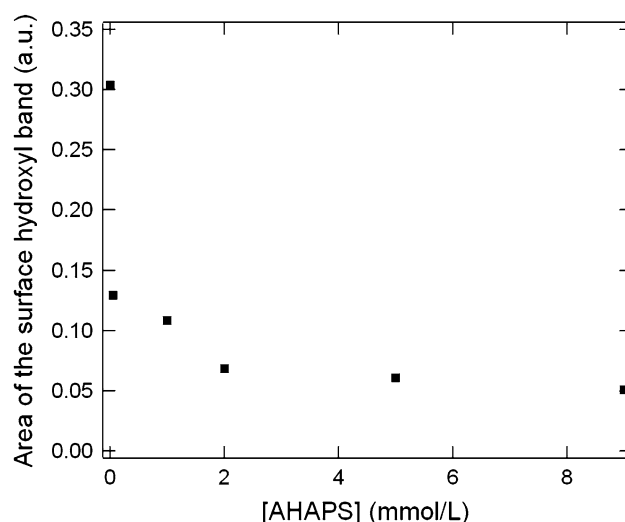
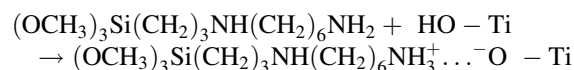


Fig. 3 Influence of the initial AHAPS concentration on the area of the infrared absorption band corresponding to surface hydroxyl groups on the TiO₂ surface (at 3,600–3,400 cm⁻¹)

suggests that the surface is saturated, in terms of chemisorbed molecules, with an initial AHAPS concentration larger than or equal to 2 mM.

However, it is expected that the system is a mixture of physisorbed and chemisorbed molecules. The physisorption mechanism is given by Ukaji et al. (2007) and Zhao et al. (2011):



The amine group takes part in the adsorption process, and the NH₃⁺ group can be monitored. The spectra in presence of AHAPS indicate a characteristic peak at ca. 1,446 cm⁻¹ (Fig. 2). This peak is frequently assigned to the pyridinium cations during the pyridine adsorption on Lewis acid sites (Herrero et al. 1991; Billingham et al. 1996; Lercher et al. 1996; Tanga et al. 2010). Following this approach, a peak at 1,446 cm⁻¹ indicates, in our work, the presence of NH₃⁺ groups on the surface. The height of the peak at 1,446 cm⁻¹ is directly connected to the initial concentration of AHAPS but is also sensitive to the titania amount. The FTIR spectra can be used to estimate, semi-quantitatively, the amount of AHAPS molecules physisorbed at the surface of titania. For that purpose, the ratio of heights ρ_1 ($\rho_1 = H_{1446}/H_{720}$) for two absorption peaks is calculated. The first one at around 1,446 cm⁻¹ is attributed to NH₃⁺ groups generated by AHAPS physisorption. The second one at 720 cm⁻¹ is typical to the Ti–O and Ti–O–Ti bonding of titania (Chen and Yakovlev 2010). In order to confirm the trend, another peak is used as quantitative reference of titania. The peak at 1,630 cm⁻¹ is attributed to stretching of –OH groups present in the titania powder. In this second case, the ratio of absorption heights

ρ_2 ($\rho_2 = H_{1446}/H_{1630}$) is also reported. Figure 4 depicts the influence of the AHAPS initial concentration on the two ratios of absorption heights ρ_1 and ρ_2 . The two curves show a similar trend. A continuous increase of ρ with the initial AHAPS concentration occurs. Note that no plateau can be observed. The absence of such a plateau suggests that the surface is not saturated with an initial AHAPS concentration larger than 9 mM.

Based on these preliminary results, it can be concluded that both physisorption and chemisorption occurs but they display a different behavior. Up to a concentration of 2 mM, a mixture of physisorption and chemisorption takes place. For larger concentrations, the chemisorbed amount remains constant while the physisorbed uptake increases. However, this approach needs to be consolidated with another quantitative one. For that reason the XPS technique is used to estimate the quantity of AHAPS adsorbed and to gain a better understanding of the sorption mechanism (chemisorption and physisorption).

3.2 XPS results and discussion

XPS is a sensitive tool for the analysis of the chemical composition of materials. Quantitative XPS analysis is performed on bare and modified TiO_2 particles to analyze the changes on the surface of TiO_2 particles by the AHAPS sorption and the nature of bonds at the oxide surface. Figure 5a is the typical XPS spectrum of the TiO_2 nanoparticles before grafting. According to the survey spectrum, the elements O, Ti, N and C are detected. The typical peaks of O 1s at 529.7 eV, Ti 2p at 458.5 eV, N 1s at 399.4 eV, and C 1s at 284.6 eV appear. The peaks of

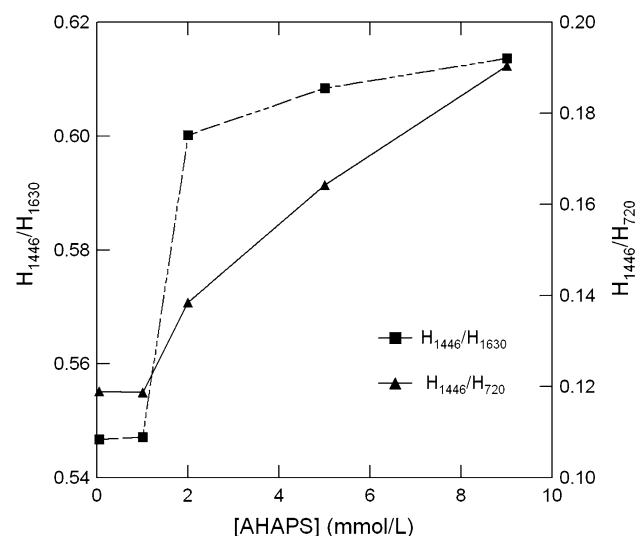


Fig. 4 Variation of the ratios of absorption heights ($\rho_1 = H_{1446}/H_{1630}$ and $\rho_2 = H_{1446}/H_{720}$) with the initial AHAPS concentration. The lines are drawn to guide the eye

nitrogen (N 1s) and carbon (C 1s) result from traces of nitrogen adsorbed on the surface and also hydrocarbon contamination. The survey spectrum of modified particles (Fig. 5b) also contains Si 2p (at 101.3 eV) and NH_3^+ (at 401.1 eV) peaks in addition to the previously observed peaks, confirming the presence of AHAPS surface modifier. The influence of the AHAPS initial concentration on the atomic percentage of Si 2p, N 1s (NH_2 and NH_3^+) and Ti 2p is reported in Table 1. Note that each value reported in the table is an average of three measurements. The table also contains the ratios of the atomic percentages of silicon to titanium (Si/Ti) and nitrogen to silicon (N/Si). As expected, the ratio Si/Ti increases with the initial AHAPS concentration. During the particle modification, no significant change of the Ti 2p content is observed while the Si 2p content increases. This indicates that the adsorption of AHAPS increases continuously with the AHAPS concentration.

Another way to track the mechanism of AHAPS sorption is to evaluate the ratio N/Si. In this case, the total atomic percentage of nitrogen (N 1s) is the sum of the

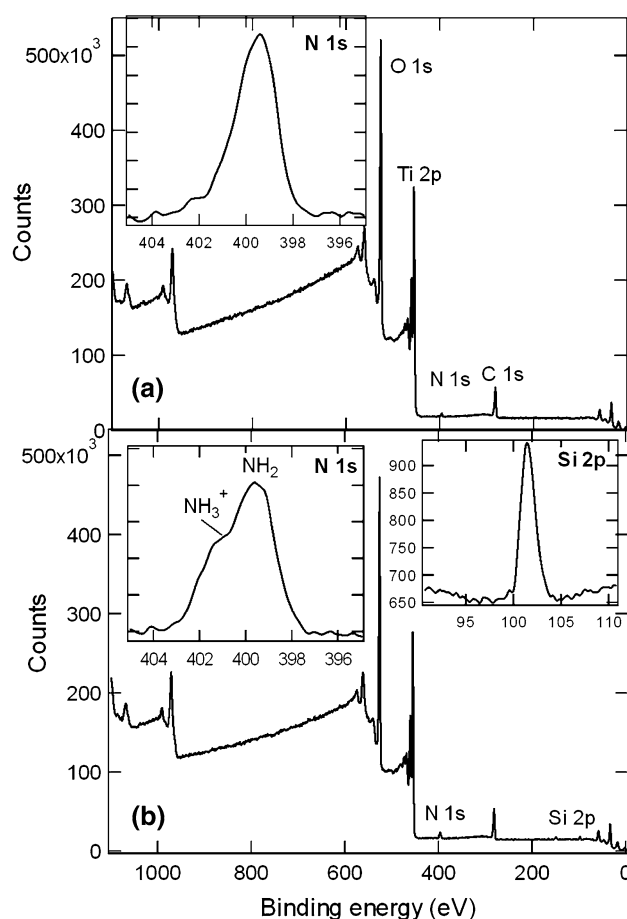


Fig. 5 XPS survey spectrum of **a** bare and **b** modified TiO_2 prepared at 9 mM initial AHAPS concentration. The insets show the binding energy spectra of N 1s and Si 2p

Table 1 Influence of the AHAPS concentration [AHAPS] on the atomic percentages and atomic ratios, obtained from X-ray photoelectron spectra, emitted by the elements (Si, N, and Ti) encountered on the surface of bare and modified TiO₂

[AHAPS] (mM)	Atomic percentage (%) Si 2p	Atomic percentage (%) N 1s	Atomic percentage (%) Ti 2p	Atomic ratio N/Si	Atomic ratio Si/Ti
0	<0.4	1.5	22.9	–	–
0.05	0.7	1.7	22.7	2.39	0.033
0.5	0.8	1.8	22.7	2.31	0.034
1	1.1	2.3	22.1	2.12	0.049
3	1.2	2.4	22.3	1.99	0.054
9	1.7	2.4	20.8	1.40	0.083

atomic percentage of NH₂ and NH₃⁺. The ratio N/Si decreases with the AHAPS concentration. This result seems surprising since, theoretically, this ratio has to be equal to 2. The difference between the calculated ratios (from 2.39 to 1.4) is larger than the measurement confidence and cannot be attributed to experimental artifact. The decrease of the ratio can be explained by the photoelectron attenuation length due to the adsorbed aminosilane molecules. Making XPS data fully quantitative in the presence of an organic layer requires to deal with photoelectron attenuation length in the organic film (Wallart et al. 2005). The classical method consists of measuring the attenuation of the XPS signal (for instance the Si 2p signal in the case of a silicon surface) after organic modification. Within the continuum model, the Si 2p signal intensity of the H-terminated (bare silicon surface, H) and modified surface (ML) is given by (Fadley 1984):

$$S_{\text{Si}}^{\text{H}} = KA_{90}\sigma_{\text{Si}2\text{p}}\rho_{\text{Si}}\lambda_{\text{Si}}(E_{\text{Si}2\text{p}}) \quad (3)$$

$$S_{\text{Si}}^{\text{ML}} = KA_{90}\sigma_{\text{Si}2\text{p}}\rho_{\text{Si}}\lambda_{\text{Si}}(E_{\text{Si}2\text{p}})\exp\left[-\frac{d}{\lambda_{\text{ML}}(E_{\text{Si}2\text{p}})\times\sin\theta}\right] \quad (4)$$

where K is an instrumental constant, A₉₀ the circular surface area analyzed for the takeoff angle $\theta = 90^\circ$, $\sigma_{\text{Si}2\text{p}}$ the photoionization cross section for Si 2p photoelectrons, ρ_{Si} the atomic volume density in silicon, d the monolayer thickness, and θ the polar angle. $\lambda_{\text{ML}}(E_{\text{Si}2\text{p}})$ and $\lambda_{\text{Si}}(E_{\text{Si}2\text{p}})$ are, respectively, the attenuation lengths of Si 2p photoelectrons in the organic monolayer and in the silicon.

Dividing Eq. (4) by Eq. (3) yields the attenuation of the Si 2p signal (A_{Si}):

$$A_{\text{Si}} = \frac{S_{\text{Si}}^{\text{ML}}}{S_{\text{Si}}^{\text{H}}} = \exp\left[-\frac{d}{\lambda_{\text{ML}}(E_{\text{Si}2\text{p}})\times\sin\theta}\right] \quad (5)$$

It is then possible to anticipate the attenuation of the Si 2p signal after AHAPS chemisorption since the Si takes part in the grafting process. In other words, the Si remains close to the surface (due to Ti–O–Si bond) while the amine group is pointed away from the surface. In the case of pure chemisorption, the ratio N/Si becomes larger than or equal to 2 since the Si 2p signal intensity is underestimated. On the

contrary, when physisorption occurs, special interaction between amino group and TiO₂ happens. The main type of interaction between aminosilane and TiO₂ is due to the formation of an ionic bonding between the protonated amine of the ligand and a negatively charged surface hydroxyl group ((OCH₃)₃Si(CH₂)₃ NH(CH₂)₆NH₃⁺...[−]OTi). The amine group takes part in the adsorption process, and the Si group points away from the surface. Consequently, the ratio N/Si appears lower than 2 because the NH₃⁺ signal intensity is underestimated. However, in our study, the system contains a mixture of physisorbed and chemisorbed molecules rather than individual substances. The ratio N/Si remains larger than 2 for AHAPS concentration lower than or equal to 1 mM. This may more likely reflect the excess of chemisorbed molecules. On the other hand, the ratio becomes lower than or equal to 2 for larger AHAPS concentrations (3–9 mM) indicating that the main contribution to the adsorption is due to physisorbed molecules. This approach should obviously be considered as a first approximation, since the system is a mixture of chemisorbed and physisorbed molecules. A rigorous theory should assume multicomponent mixture of chemisorbed and physisorbed molecules.

The distinction between different type of nitrogen atoms by XPS (NH₂ at 399.3 eV and NH₃⁺ at 401.2 eV), allows us to distinguish between physisorbed and chemisorbed molecules on the surface. It seems more convenient to estimate the percentage of physisorbed and chemisorbed molecules onto the surface. The percentage of AHAPS physisorbed molecules (%Physisorption) is defined by:

$$\% \text{Physisorption} = 2 \times \frac{\text{NH}_3^+ \times \text{N}}{100 \times \text{Ti}} \quad (6)$$

where NH₃⁺ and Ti are the atomic percentages of NH₃⁺ and titanium, respectively. The total atomic percentage of nitrogen (N) is the sum of the atomic percentages of NH₂, NH and NH₃⁺.

The expression $\frac{\text{NH}_3^+ \times \text{N}}{100 \times \text{Ti}}$ gives the contribution of the atomic percentage of NH₃⁺ normalized by the Ti amount on the surface. However, the AHAPS molecule contains 2N atoms (NH₃⁺ and NH) or, in other words, each NH₃⁺ atom is coupled to a NH group. Then, if we would like to

obtain the percentage of AHAPS physisorbed molecules (%physisorption) it becomes necessary to multiply by a factor 2.

The percentage of AHAPS chemisorbed molecules (%chemisorption) can be written as:

$$\% \text{Chemisorption} = \frac{N \times (\text{NH}_2, \text{NH})}{100 \times \text{Ti}} - \frac{\% \text{Physisorption}}{2} \quad (7)$$

where (NH₂, NH) denotes the atomic percentage of NH and NH₂. The ratio $\frac{N \times (\text{NH}_2, \text{NH})}{100 \times \text{Ti}}$ represents the contribution of the atomic percentage of all the NH and NH₂ atoms normalized by the Ti amount on the surface. However, the AHAPS molecules contain 2N atoms. It is then necessary to eliminate the contribution of the NH group corresponding to the physisorbed molecules which is given by $\frac{\% \text{Physisorption}}{2}$.

Figure 6 shows the dependence on the initial AHAPS concentration of the percentage of physisorbed and chemisorbed molecules on titania. The two curves show different trend. The physisorbed amounts are much higher than the chemisorbed amounts. A continuous increase of the percentage of physisorbed molecules with the concentration is observed. Another interesting feature in the figure is that the chemisorbed amount reaches a plateau in the very first part of the isotherm, at AHAPS concentration about 0.05 mM. The physisorbed uptake depends highly on the AHAPS concentration while the chemisorbed amount remains constant. The XPS adsorption trend is similar to that previously described using FTIR analysis (Figs. 3, 4). The concordance between the two series of data does also somehow validate the analytical procedures, more specifically the acknowledged difficult semi-quantitative FTIR approach. As far as the physisorption is concerned, the XPS data take into account the two modes of physisorption (hydrogen bonding and ionic bonding) while the FTIR approach considers only the ionic bonding between the basic amine and a surface hydroxyl group. The similarity between XPS measurements and FTIR analysis suggests that the main physisorption mechanism is the ionic bonding between the basic amine and a surface hydroxyl group. However, previous FTIR analysis had shown that the amount of chemisorbed molecules became constant for an AHAPS concentration of 2 mM. The concentration for which the chemisorption reach saturation seems affected by the characterization technique, i.e. 0.05 mM (XPS) or 2 mM (FTIR). The discrepancy might be caused by the experimental uncertainties or it may more likely reflect the XPS quantitative simplification. Recall that the photoelectron attenuation length was neglected in the XPS quantitative analysis despite the presence of the organic layer.

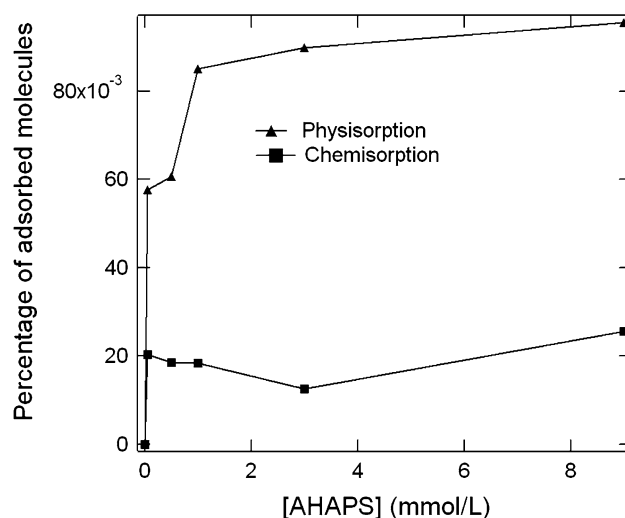


Fig. 6 Percentage of AHAPS physisorbed molecules (“Physisorption”, triangles) and chemisorbed molecules (“Chemisorption”, squares) as a function of the initial AHAPS concentration. The percentage of physisorbed molecules is calculated, from the XPS data, using Eq. (6) while the percentage of chemisorbed molecules is obtained using Eq. (7). The lines are drawn to guide the eye

3.3 Low-pressure argon and nitrogen adsorption

Quasi-equilibrium gas adsorption experiments are performed at 77 K, and the distributions of adsorption energy are calculated from the derivative adsorption isotherms. The DIS method is set for the decomposition of isotherm derivative curves into many local isotherms or energy peaks. It enables us to follow the evolution of the surface heterogeneity in the course of the surface modification. Argon is an inert and nonpolar gas which interacts with adsorbent sites by van der Waals–London interactions and thus is mainly sensitive to geometric features of solids. On the contrary, nitrogen is a bimolecular gas which interacts with adsorbent sites by both van der Waals–London interactions and Debye interactions. It is thus useful for evaluating the polar–apolar nature of the solid surface.

Quasi-equilibrium Ar derivative adsorption isotherms obtained for bare and modified samples are presented in Fig. 7. The figure also contains the corresponding fits using the DIS procedure. The related modeling parameters are collected in Table S1 of the Supplementary Material. Five adsorption domains can be defined as shown in Fig. 7. Three main contributions can be extracted: domains 2, 3, and 4 located at $\ln(P/P_0)$ values of -10.3 , -7.5 , and -5.3 , respectively. The domain 1 centered around $\ln(P/P_0) = -13.6$ is hardly distinguishable. This high-energy adsorption domain is in relation to more undercoordinated surface atoms or surface defects that display high energy (Ali Ahmad et al. 2012). For the domain of very low energy (domain 5 located at $\ln(P/P_0) = -2.3$), one may notice that

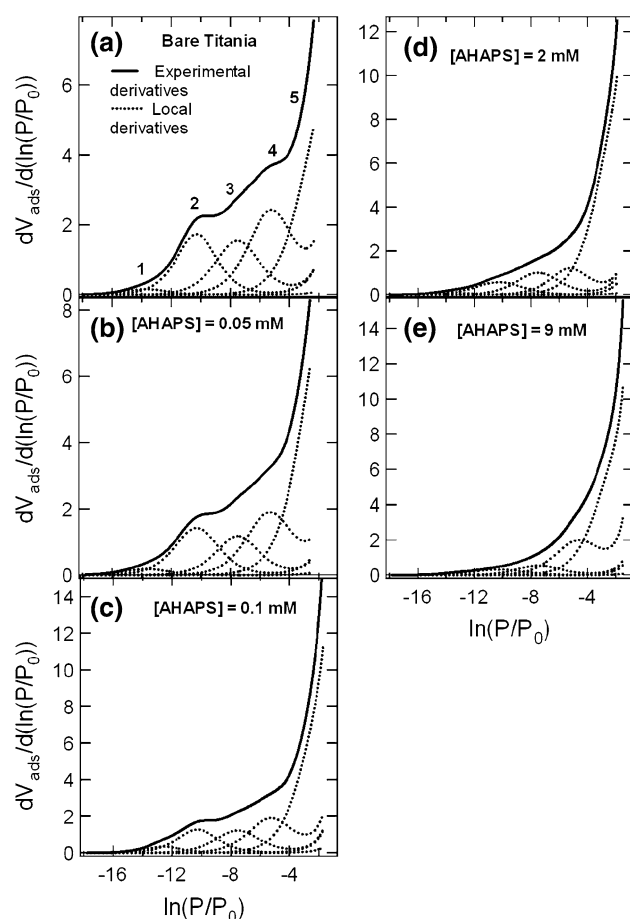


Fig. 7 DIS modeling of argon derivative isotherms recorded at 77 K onto **a** bare titania, titania modified with AHAPS at **b** 0.05 mM, **c** 0.1 mM, **d** 2 mM, and **e** 9 mM

its contribution increases with the AHAPS adsorbed amount. The derivation leads to an exponential shape for the derivative curves typical of low-energy solid surfaces (Villieras et al. 2007; Ruckriem et al. 2010; Stephanovic et al. 2010).

Considering the relative amount of each domain (a proportion calculated from the V_m parameter, Table S1 of the Supplementary Material), the peaks located in the domains 2, 3, and 4 (located at $\ln(P/P_0)$ values of -10.3 , -7.5 , and -5.3 , respectively) represent the main contribution to the energy distribution. These domains are assigned to crystallographic faces of anatase titania according to previous results obtained by Ali Ahmad et al. (2012). On the one hand, it is reasonable to ascribe the domains 2 and 3 at $\ln(P/P_0)$ values of -10.3 and -7.5 to the presence of the $\{101\}$ face at the nanoparticles surface. On the other hand, the $\{001\}$ face is related to the domain 4 centered around $\ln(P/P_0) = -5.3$.

Based on this assumption it becomes possible to follow the evolution of the DIS specific area of the $\{101\}$ face ($S(101)$) and the $\{001\}$ face ($S(001)$) versus the initial

AHAPS concentration (Table 2). The table contains also the ratio of the specific areas ($S(101)/S(001)$). The evolution of the specific area for the $\{101\}$ and $\{001\}$ faces are quite similar. There is a decrease of the specific area with the AHAPS concentration. The specific areas of bare titania are equal to 46 and 35 m^2/g for $S(101)$ and $S(001)$, respectively, and they decrease up to a value of 14 and 10 m^2/g at a AHAPS concentration of 9 mM. The AHAPS molecules are mostly located on the $\{101\}$ and $\{001\}$ faces. The AHAPS concentration has no influence on the ratio $S(101)/S(001)$. The average value equals 1.36 ± 0.09 . This result clearly establishes that the two faces display the same reactivity toward AHAPS sorption. This is a very important result because other studies pointed out that the adsorption or the grafting of organic molecules is largely influenced by the nature of the crystallographic faces. An example was described by Villieras et al. (2007) for the grafting of silicones on calcium carbonate and by Stephanovic et al. (2010) in the case of pyridine adsorbing on goethites. This is not the case in the present study. Note also that for AHAPS concentration of 9 mM, the specific areas $S(101)$ and $S(001)$ are not equal to 0 ($S(101) = 14 \text{ m}^2/\text{g}$ and $S(001) = 10 \text{ m}^2/\text{g}$). Such remaining specific area indicates that the titania is not fully covered with AHAPS molecules.

Molecular nitrogen is usually considered as a Lewis base, and it is thus useful for evaluating the polar–apolar nature of the solid surface. Figure 8 and Table S2 (Supplementary Material) present the quasi-equilibrium nitrogen derivative adsorption isotherms together with their DIS decomposition obtained for bare and modified samples. For all the derivative isotherms, no less than seven domains are needed for a good fit (Fig. 8). Each decomposition results in three high energy domains (domains 1–3), 3 medium energy domains (domains 4–6) and one low energy domain (domain 7 located at around $\ln(P/P_0) = -2.6$).

It can be noticed that the main adsorption domain is located at a high-energy value ($-16 < \ln(P/P_0) < -13$). This domain is centered in most cases at a $\ln(P/P_0)$ around -14.3 and recomposed using three local derivative isotherms (domains 1, 2, and 3). In the case of nonpolar surfaces, the difference in peak positions between argon and nitrogen should correspond to a $\ln(P/P_0 \text{ Ar}) - \ln(P/P_0 \text{ N}_2)$ around 1.3 (Bégin-Colin et al. 2009). In the present case, the shift of the peak at a high energy from $\ln(P/P_0) = -10.2$ for argon to -14.3 for nitrogen is much higher than 1.3. This indicates the presence of polar surface sites on the surface of the sample. This difference in peak positions is better reproduced ($\ln(P/P_0 \text{ Ar}) - \ln(P/P_0 \text{ N}_2) = 1.3$) for other domains around -9.1 , -6.2 , and -2.6 , at medium and low energies, and can be assigned to apolar surface sites.

The amount of gas adsorbed (V_m) on the high-energy sites decreases with the AHAPS concentration whereas the

Table 2 Influence of the AHAPS concentration ([AHAPS]) on the DIS specific area of the {101} face (S(101)) and the {001} face (S(001))

[AHAPS] (mM)	0	0.05	0.1	2	9
S(101) (m ² /g)	46.88	38.19	36.05	25.09	14.30
S(001) (m ² /g)	35.43	28.44	27.85	16.35	10.83
S(101)/S(001)	1.32	1.34	1.29	1.53	1.33

The specific areas are obtained from DIS modeling parameters for argon adsorption onto bare and modified TiO₂. The domains 2 and 3 at $\ln(P/P_0)$ values of -10.3 and -7.5 correspond to the {101} face at the nanoparticles surface while the {001} face is related to the domain 4 centered at around $\ln(P/P_0) = -5.3$

amount adsorbed on medium and low energy sites appear roughly constant regardless of the ligand concentration. This evidences that the AHAPS sorption occurs mainly on the polar high-energy adsorption domains. In the following, the peaks located in the domains 1, 2 and 3 are only considered. To confirm this assumption, it is interesting to follow up the evolution of the DIS specific area of the high-energy domains which occurs in the course of the chemical reaction. More precisely, the evolution of the DIS specific area of the high-energy domains is compared with the

AHAPS adsorbed amount, obtained from XPS analysis (ratio Si/Ti, Fig. 9). The specific area is the sum of the DIS area of the domains 1, 2 and 3. The specific area decreases linearly with the quantity adsorbed of AHAPS on titania surface. The evolution of the DIS specific area is in good agreement with the ligand adsorbed amount. The similarity between data demonstrates that the diminution of the specific area is due to the AHAPS adsorption. This confirms that the AHAPS sorption occurs mainly on the three sites of high energy.

To assign the local adsorption domains to AHAPS sorption mechanism (chemisorption and physisorption), the variation of the DIS specific area, for each domain, in the course of the chemical reaction is calculated. Figure 10 presents the evolution of the percentage of change of the specific area on the different sites of high-energy as a function of the AHAPS concentration. For each site, the specific area decreases with the concentration. It appears that the specific area of the site corresponding to domain 1 (located at $\ln(P/P_0) = -15.8$) follows the pattern already

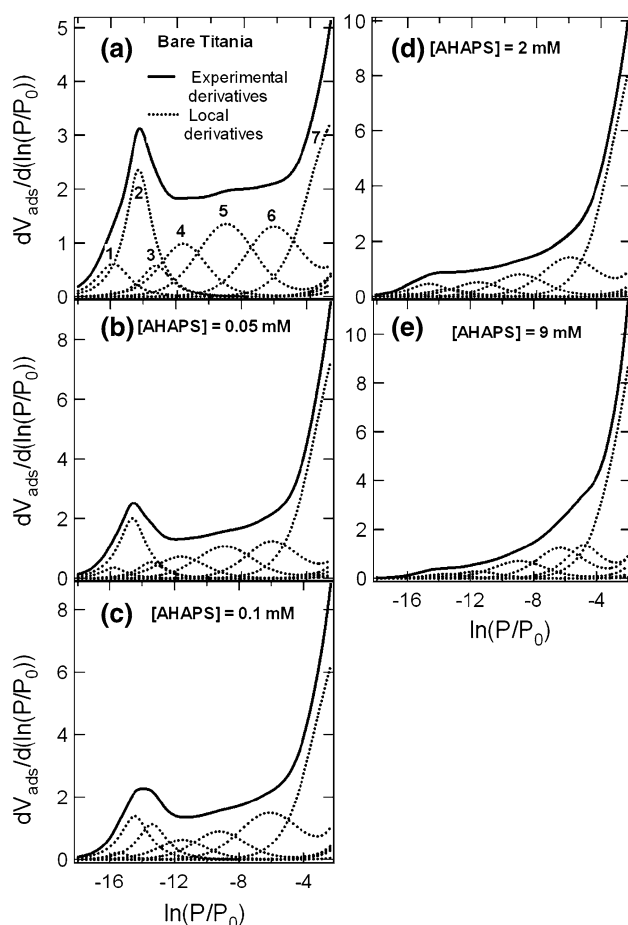


Fig. 8 DIS modeling of nitrogen derivative isotherms recorded at 77 K onto **a** bare titania, titania modified with AHAPS at **b** 0.05 mM, **c** 0.1 mM, **d** 2 mM, and **e** 9 mM

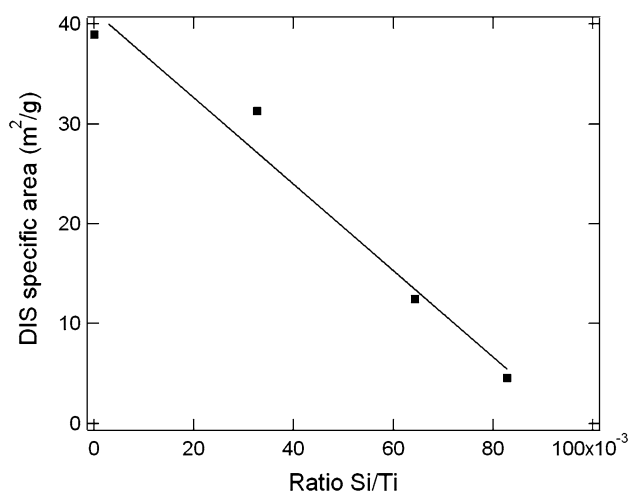


Fig. 9 Correlation between data obtained by low-pressure nitrogen adsorption (DIS specific area) and XPS measurements (Ratio Si/Ti). The DIS specific area is the sum of the area of the domains 1, 2 and 3. The ratio Si/Ti denotes the ratio of the atomic percentages of silicon to titanium (Si/Ti) obtained from XPS analysis (Table 1). The line represents the best linear fit given by $S = -432.5 (\text{Si/Ti}) + 41.2$ ($R^2 = 0.968$)

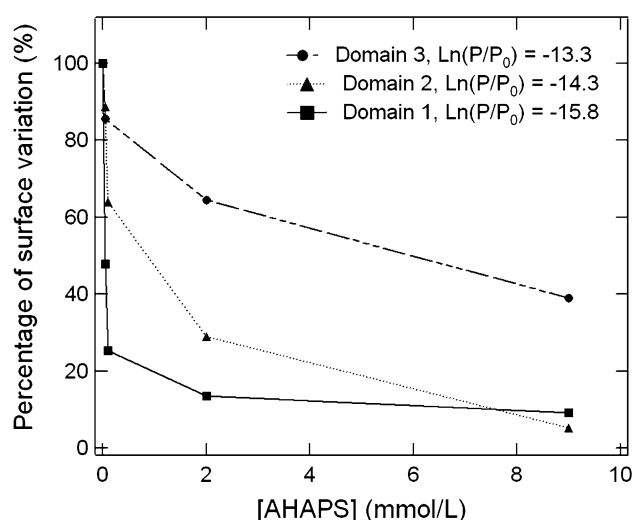


Fig. 10 Influence of the AHAPS concentration on the variation of the percentage of change of the DIS specific area on the different sites of high-energy. The DIS specific areas are obtained from DIS modeling parameters for nitrogen adsorption onto bare and modified TiO₂. The lines are drawn to guide the eye

observed for the chemisorbed amount (Figs. 3, 6): initial significant decrease up to 0.1 mM followed by a plateau. Note that the plateau previously observed in XPS and FTIR analysis can be observed. The similarity between volumetry measurements and XPS/FTIR analysis suggests that the chemisorption occurs mainly on the adsorption domain 1. This domain displays the highest energy and it seems logical that the chemisorption occurs preferentially on this domain. For the two other domains (domains 2 and 3) the decrease of the percentage of change of the specific area is continuous but less pronounced. They follow the trend previously reported for the AHAPS physisorption (Figs. 4, 6). Consequently, the AHAPS molecules are preferentially physisorbed on the domains 2 and 3. To summarize, the AHAPS sorption takes place on polar domains with high-energy. The molecules are chemisorbed onto the site of highest energy while they are physisorbed on the following lower energy sites.

4 Conclusion

In this study, an aminosilane coupling agent AHAPS is applied as a particle surface modifier of TiO₂ nanoparticles. The main objective of this article is to highlight the importance of the physisorption during the aminosilane grafting process on titania. For this purpose, the evolution of the chemisorbed and physisorbed aminosilane molecules on TiO₂ is thoroughly analyzed. The concentration of AHAPS in the reaction solution has been varied to obtain different surface coverage of AHAPS on TiO₂. Several measurements have been made on solid samples in order to

characterize the modification of the titania surface: FTIR, XPS and low-pressure argon and nitrogen adsorption.

The adsorption data obtained from FTIR analysis compare very well with those of XPS measurements. The combination of these two techniques allows the determination of the chemisorbed and physisorbed contribution. The results demonstrate that the aminosilane creates an adsorbed layer containing a mixture of physisorbed and chemisorbed molecules. The physisorbed amount is dominant regardless of the AHAPS concentration (0.05–9 mM). The aminosilane physisorption makes a major contribution in the composition of the interface, and consequently, it plays a significant role in the grafting efficiency. In the case of aminosilane concentration effect, the physisorbed uptake increases with the initial AHAPS concentration whereas the chemisorbed amount remains roughly constant. More precisely, the chemisorbed AHAPS increases with silane concentration up to the formation of a plateau for an initial concentration of 0.05 mM (XPS) or 2 mM (FTIR) depending on the experimental method.

Quantitative information on surface energy of TiO₂, in terms of adsorption energy sites and heterogeneity, has been investigated by quasi-equilibrium low-pressure adsorption technique. By using argon and nitrogen as probe molecules, it is possible to correlate the titania surface structure with its reactivity toward AHAPS adsorption. The DIS data treatment applied to argon adsorption results in the evaluation of the surface areas of the crystallographic faces exposed on the TiO₂ surface and their respective proportion. The AHAPS molecules are mainly located on the {101} and {001} faces of titania. More interestingly, the two faces present an equivalent reactivity toward AHAPS sorption. Nitrogen adsorption experiments, supported by appropriate modeling approach, clearly evidence the presence of polar surface sites. The AHAPS adsorption takes place on the three polar surface sites of high energy. The chemisorbed silane is adsorbed via covalent bond onto the site displaying the highest energy. Conversely, the AHAPS molecules are physisorbed on the two lower energy sites.

It is also interesting to compare the surface modification of TiO₂ nanoparticles with AHAPS and APTES. Similar adsorption trends are observed with APTES. The APTES attachment on TiO₂ occurs far from an ideally oriented chemisorbed monolayer. More than 50 % of the APTES molecules show reverse attachment (physisorption) which is due to the coordination of the APTES amino group on the titania. In addition, the amount and the APTES orientation (chemisorption or physisorption) depend on the crystal structure of the substrate. Physisorption is more pronounced on rutile than on anatase surfaces.

Reported results provide useful guidelines for the grafting of aminosilanes on inorganic particles. This work

suggests that the physisorption is a key parameter during the aminosilanes grafting process. To efficiently control the chemical grafting of aminosilanes and correlated properties, physisorption must be taken into account. In order to significantly remove the molecules physisorbed thorough rinsing has to be performed at the end of the grafting process.

Acknowledgments We express our gratitude to Dr. Aurélien Renard and Martine Mallet (LCPME, Université de Lorraine, CNRS) for acquiring the XPS spectra.

References

- Aldeek, F., Mustin, C., Balan, L., Roques-Carmes, T., Fontaine-Aupart, M.P., Schneider, R.: Surface-engineered quantum dots for the labeling of hydrophobic microdomains in bacterial biofilms. *Biomaterials* **32**, 5459–5470 (2011)
- Ali Ahmad, M., Prelot, B., Razafitianamaharavo, A., Douillard, J.M., Zajac, J., Dufour, F., Durupthy, O., Chaneac, C., Villiéras, F.: Influence of morphology and crystallinity on surface reactivity of nanosized anatase TiO₂ studied by adsorption techniques. 1. The use of gaseous molecular probes. *J. Phys. Chem. C* **116**, 24596–24606 (2012)
- Bégin-Colin, S., Gardalla, A., Le Caer, G., Humbert, O., Thomas, F., Barres, O., Villiéras, F., Toma, L.F., Bertrand, G., Zahraa, O., Gallart, M., Hönerlage, B., Gilliot, P.: On the origin of the decay of the photocatalytic activity of TiO₂ powders ground at high energy. *J. Phys. Chem. C* **113**, 16589–16602 (2009)
- Billingham, J., Breen, C., Yarwood, J.: In situ determination of Bronsted/Lewis acidity on cation-exchanged clay mineral surfaces by ATR-IR. *Clay Miner.* **31**, 513–522 (1996)
- Blin, J.L., Stébé, M.J., Roques-Carmes, T.: Use of ordered mesoporous titania with semi-crystalline framework as photocatalyst. *Colloids Surf. A* **407**, 177–185 (2012)
- Bowen, P.: Particle size distribution measurement from millimeters to nanometers and from rods to platelets. *J. Disper. Sci. Technol* **23**, 631–662 (2002)
- Brandow, S.L., Chen, M.S., Aggarwal, R., Dulcey, C.S., Calvert, J.M., Dressick, W.J.: Fabrication of patterned amine reactivity templates using 4-chloromethylphenylsiloxane self-assembled monolayer films. *Langmuir* **15**, 5429–5432 (1999)
- Brunette, D., Tengvall, P., Textor, M., Thomsen, P.: *Titanium in Medicine: Material Science, Surface Science, Engineering, Biological Responses and Medical Applications*. Springer, Heidelberg (2001)
- Chen, Q., Yakovlev, N.L.: Adsorption and interaction of organosilanes on TiO₂ nanoparticles. *Appl. Surf. Sci.* **257**, 1395–1400 (2010)
- Durupthy, O., Bill, J., Aldinger, F.: Bioinspired synthesis of crystalline TiO₂: effect of amino acids on nanoparticles structure and shape. *Cryst. Growth Des.* **7**, 2696–2704 (2007)
- Fadley, C.S.: Angle-resolved X-ray photoelectron spectroscopy. *Prog. Surf. Sci.* **16**, 275–388 (1984)
- Grätzel, M.: Photoelectrochemical cells. *Nature* **414**, 338–344 (2001)
- Harnett, C.K., Satyalakshmi, K.M., Craighead, H.G.: Bioactive templates fabricated by low-energy electron beam lithography of self-assembled monolayers. *Langmuir* **17**, 178–182 (2001)
- Herrero, J., Pajares, J.A., Blanco, C.: Surface acidity of palygorskite-supported rhodium catalysts. *Clays Clay Miner.* **39**, 651–657 (1991)
- Herrmann, J.M.: Photocatalysis fundamentals revisited to avoid several misconceptions. *Appl. Catal. B Environ.* **99**, 461–468 (2010)
- Hoogeveen, N., Cohen Stuart, M.A., Fler, G.J.: Polyelectrolyte adsorption on oxides II. Reversibility and exchange. *J. Colloid Interface Sci.* **182**, 146–157 (1996)
- Jansson, M., Jonsson, M., Mohl, J.: Kinetic evaluation of sorption and desorption. *Adsorption* **16**, 155–159 (2010)
- Kneuer, C., Sameti, M., Haltner, E.G., Schiestel, T., Schirra, H., Schmidt, H., Lehr, C.M.: Silica nanoparticles modified with aminosilanes as carriers for plasmid DNA. *Int. J. Pharm.* **196**, 257–261 (2000)
- Lazghab, M., Saleh, K., Guigon, P.: Fonctionnalisation of porous silica powders in a fluidized-bed reactor with glycidoxypolytrimethoxysilane (GPTMS) and aminopropyltriethoxysilane (APTES). *Chem. Eng. Res. Des.* **88**, 686–692 (2010)
- Lee, S.H., Saito, N., Takai, O.: Self-assembly of human plasma fibrinogens on binary organosilane monolayers with micro domains. *Appl. Surf. Sci.* **255**, 7912–7917 (2009)
- Lercher, J.A., Grundling, C., Eder-Mirth, G.: Infrared studies of the surface acidity of oxides and zeolites using adsorbed probe molecules. *Catal. Today* **27**, 353–376 (1996)
- Michot, L.J., François, M., Cases, J.M.: Surface heterogeneity studied by a quasi-equilibrium gas adsorption procedure. *Langmuir* **6**, 677–681 (1990)
- Oh, S.J., Cho, J.C., Kim, C.O., Park, J.W.: Characteristics of DNA microarray fabricated on the various aminosilane layers. *Langmuir* **18**, 1764–1769 (2002)
- Petri, D.S., Wenz, G., Schunk, P., Schimmel, T.: An improved method for the assembly of amino-terminated monolayers on SiO₂ and the vapor deposition of gold layers. *Langmuir* **15**, 4520–4523 (1999)
- Prelot, B., Villiéras, F., Pelletier, M., Gérard, G., Gaboriaud, F., Ehrhardt, J.J., Perrone, J., Fedoroff, M., Jeanjean, J., Lefèvre, G.: Morphology and surface heterogeneities in synthetic goethites. *J. Colloid Interface Sci.* **261**, 244–254 (2003)
- Roques-Carmes, T., Membrey, F., Kaisheva, M., Filiâtre, C., Foissy, A.: Reflectometric study of the adsorption of poly(vinyl imidazole) on a gold electrode, effects of pH, and applied potential. *J. Colloid Interface Sci.* **299**, 504–512 (2006)
- Ruckriem, M., Inayat, A., Enke, D., Glaser, R., Einicke, W.D., Rockmann, R.: Inverse gas chromatography for determining the dispersive surface energy of porous silica. *Colloids Surf. A* **357**, 21–26 (2010)
- Stephanovic, S., Ali Ahmad, M., Razafitianamaharavo, A., Villiéras, F., Barrès, O., Prelot, B., Zajac, J., Douillard, J.M., Chanéac, C.: Evidences for the relationship between surface structure and reactivity of goethite nanoparticles based on advanced molecular-probe methods. *Adsorption* **16**, 185–195 (2010)
- Tanga, X., Li, J., Suna, L., Hao, J.: Origination of N₂O from NO reduction by NH₃ over β-MnO₂ and α-Mn₂O₃. *Appl. Catal. B* **99**, 156–162 (2010)
- Ukaji, E., Furusawa, T., Sato, M., Suzuki, N.: The effect of surface modification with silane coupling agent on suppressing the photo-catalytic activity of fine TiO₂ particles as inorganic UV filter. *Appl. Surf. Sci.* **254**, 563–569 (2007)
- Vandenberg, E.T., Bertilsson, L., Liedberg, B., Uvdal, K., Erlandsson, R., Elwing, H., Lundstroem, I.: Structure of 3-aminopropyl triethoxy silane on silicon oxide. *J. Colloid Interf. Sci.* **147**, 103–118 (1991)
- Villiéras, F., Cases, J.M., François, M., Michot, L.J., Thomas, F.: Texture and surface energetic heterogeneity of solid from modeling of low pressure gas adsorption isotherms. *Langmuir* **8**, 1789–1795 (1992)
- Villiéras, F., Michot, L.J., Bardot, F., Cases, J.M., François, M., Rudzinski, W.: An improved derivative isotherm summation

- method to study surface heterogeneity of clay minerals. *Langmuir* **13**, 1104–1117 (1997)
- Villieras, F., Leboda, R., Charmas, B., Bardot, F., Gérard, G., Rudzinski, W.: High resolution argon and nitrogen adsorption of the surface heterogeneity of carbosils. *Carbon* **36**, 1501–1510 (1998)
- Villieras, F., Michot, L.J., Bardot, F., Chamerois, M., Eypert-Blaison, C., François, M., Gérard, G., Cases, J.M.: Surface heterogeneity of minerals. *C. R. Geosci.* **334**, 597–609 (2002)
- Villieras, F., Chamerois, M., Yvon, J., Cases, J.M.: Surface heterogeneity at the solid–gas interface of hydrophilic solids modified by water-repellent molecules. *Adsorpt. Sci. Technol.* **25**, 561–571 (2007)
- Wallart, X., Henry de Villeneuve, C., Allongue, P.: Truly quantitative XPS characterization of organic monolayers on silicon: study of alkyl and alkoxy monolayers on H-Si(111). *J. Am. Chem. Soc.* **127**, 7871–7878 (2005)
- Weigel, C., Kellner, R.: FTIR-ATR-spectroscopic investigation of the silanization of germanium surfaces with 3-aminopropyltriethoxysilane. *Fresenius Z. Anal. Chem.* **335**, 663–668 (1989)
- Wu, Y.L., Lin, J.J., Hsu, P.Y., Hsu, C.P.: Highly sensitive polysilicon wire sensor for DNA detection using silica nanoparticles/ γ -APTES nanocomposite for surface modification. *Sens. Actuators B* **155**, 709–715 (2011)
- Yang, S.Q., Yuan, P., He, H.P., Qin, Z.H., Zhou, Q., Zhu, J.X., Liu, D.: Effect of reaction temperature on grafting of γ -aminopropyl triethoxysilane (APTES) onto kaolinite. *Appl. Clay Sci.* **62**, 8–14 (2012)
- Zhao, J., Milanova, M., Warmoeskerken, M.M.C.G., Dutschk, V.: Surface modification of TiO₂ nanoparticles with silane coupling agents. *Colloids Surf. A* **413**, 273–279 (2011)
- Zheng, J.W., Zhu, Z.H., Chen, H.F., Liu, Z.F.: Nanopatterned assembling of colloidal gold nanoparticles on silicon. *Langmuir* **16**, 4409–4412 (2000)